Chapter 1
History Dependent Temporal Changes of Properties of Thin Polymer Films

Günter Reiter

Abstract Despite an extensive number of investigations, it is becoming increasingly obvious that a clear understanding of thin polymer film properties has not yet been reached. The origin of (some of) the puzzling behavior of thin polymer films is still not satisfactorily unveiled. At present, we are still missing a consistent understanding of how film preparation and confinement affect film properties, in particular on approaching the glass transition temperature. While it may be disputable if the change from the initial solution to a dry glassy film introduces a "conformational state" with its "own" properties, we will present various findings, mainly observed in dewetting experiments, which demonstrate the influence of sample preparation and of the thermal history these films have undergone. We conclude that thickness is not the only parameter defining the properties of thin polymer films, i.e., they depend in addition on what happened to a film before a particular measurement was performed.

1.1 Introduction and General Aspects

Polymers represent one of the most important, versatile and strongest growing classes of materials for constructing functional systems. Polymers are thus included in a wide range of applications, e.g., as structural elements (deformable parts, lightweight matrix for composite materials, fiber materials, …) or as functional units (organic electronics, photovoltaics, optical and mechanical meta-materials, …).

Two key aspects are performance and processability. To meet future challenges in energy production and storage, medical technology, information technology and sustainable development we therefore require significant advancements in improving

G. Reiter (✉)
Institute of Physics and Freiburg Materials Research Center,
University of Freiburg, 79104 Freiburg, Germany
e-mail: guenter.reiter@physik.uni-freiburg.de

S. Napolitano (ed.), *Non-equilibrium Phenomena in Confined Soft Matter*,
Soft and Biological Matter, DOI 10.1007/978-3-319-21948-6_1

the performance of polymeric materials. At the same time, fast and efficient processing conditions are required for the production of such innovative and advanced polymeric materials. These conditions can, especially when the intrinsic molecular relaxation times are longer than the processing time, i.e., Weissenberg numbers larger than 1, determine the final properties of these materials and thus their suitability for various applications (a few examples are given in: [1–6]). Accordingly, influencing material properties by processing conditions allows to widen the range of applications as these properties may become adaptable to the needs of the application. Thus, it is essential that concepts for polymer processing change from empirically optimizing processing parameters to a rational and predictive strategy in designing the desired properties. In the here presented experimental studies on varying properties of polymers of thin films, we aim to develop some preliminary concepts for tuning properties of polymers via processing steps.

Polymers are entropy-dominated systems. During processing, these systems can evolve through different sequences of states, corresponding to different topological pathways of similar energy [3]. These pathways may involve structure formation by self-assembly, phase separation, phase transitions, etc. Small free-energy differences between these states offer the possibility to select pathways to desired morphologies that may not correspond to equilibrium. Fast processing of polymers unavoidably introduces out-of-equilibrium chain conformations because polymers cannot fully relax during the limited time allowed by processing conditions [1–6]. A multitude of possible non-equilibrium states can be established, mainly due to the chain-like structure of polymers, which allows for a vast number of possible arrangements of the monomers without risking to loose connectivity between these segments. Here, in the context of thin polymer films, we mainly concentrate on non-equilibrium states introduced by different ways of thin film preparation from rather dilute solutions and show how properties of such thin polymer films can be affected by such states.

Processing of polymers often involves a sequence of physical operations such as evaporation, temperature change or shear which will generate forces acting on the polymer chains. Under the influence of such forces, polymer chains can change their conformations, i.e., the arrangements of the connected monomers, and are thus able to exist in different states of order. Polymer conformations sensitively affect mechanical, rheological, optical, electronic properties. Taking advantage of this molecular flexibility and adaptability, even a single component polymer system may become functional and adaptable.

Recently, several research groups have begun to investigate how polymer conformations and structures topologically evolve and how this evolution could be guided during typical processing situations [1–6]. However, we still need to undertake significant efforts to identify fundamental steps during polymer processing to finally be able to actively guide structural evolution of appropriate designed materials to realize the desired functions and properties.

We may hope to improve material performance by strategically exploiting non-equilibrium preparation pathways for the formation of these complex

macromolecular systems, which includes possibilities to reduce processing time through ultra-fast processes and high throughput approaches. In addition, the long-term stability (slow aging behavior) may be enhanced through the identification and implementation of long-lived metastable non-equilibrium structures.

Thin films are often prepared from a dilute solution. Spin-casting is one of the most frequently applied techniques [7–9], yielding extremely smooth and apparently homogenous films with a thickness down to ca. 2 nm within seconds [10–14]. By varying the concentration of the solution, the process of spin-casting allows to vary easily and controllably the film thickness. In the course of spin-casting, the solvent evaporates rapidly. Due to evaporation, the concentration of the polymer within the solution increases and eventually the film vitrifies. Often, vitrification occurs already at a point when there is still a significant amount of solvent within the film. Due to the short processing time and the increasing polymer relaxation time, it is questionable if the initially swollen and significantly separated polymers are able to sufficiently interpenetrate and equilibrate in the course of film preparation.

During such processing, often significant forces are acting on a polymer chain which may respond via changes of its conformation. For a given length of a polymer, the magnitude of these changes will depend on the value of the acting force and the time scale on which this force is acting. Often the time scale of processing is much shorter than the relaxation time scales of macromolecules, which can be quite long due to the large size and a correspondingly low mobility of macromolecules. Thus, one has to expect a large spectrum of non-equilibrium states.

Presently we do not have detailed and systematic studies on how acting forces change polymer conformations and we are consequently lacking fundamental understanding for a rational design of processing steps in terms of modifying/adjusting macromolecular conformations or controlling of macromolecular conformations of non-equilibrium states. We do not possess a theoretical framework for describing non-equilibrium states of macromolecules.

A large number of studies on thin polymer films revealed that various physical properties exhibited characteristics strongly deviating from their bulk behavior [10–47], with major implications for most technological applications based on such nanoscopic films. Diverse measurements have shown anomalous irreversible and reversible density changes after annealing below the bulk glass transition temperature, unexpected instabilities of these films, unusual aging, deviations in mobility, deformed chain conformations, dewetting processes independent of molecular weight and much faster than suggested by bulk visco-elasticity, clear indications for residual stresses within these spin-coated thin polymer films, a thickness but also history dependent glass transition temperature, and fast relaxation processes. The cause of these deviations is a matter of ongoing debate.

1.2 "Historical" Remarks on Thin Polymer Films

As mentioned above, the consequences of non-equilibrium chain conformations of the polymers on film properties are not yet well understood. But we may speculate that sample preparation represents a possible cause for the anomalous behavior in glassy thin polymer films. Film preparation may have an influence on measurements of visco-elastic properties, film stability, glass transition temperature, diffusion coefficient, etc. In particular, we have to examine if fast evaporation of the solvent during the widely used process of spin-casting [7–9] can potentially affect the properties of polymer thin films.

In this context, it is instructive to have a look at some previous studies on spin-cast thin polymer films [10–13, 15–18, 47]. Being able to prepare smooth thin polymer films of variable thickness allowed to study questions related to the chain-like nature of macromolecules. In particular, it has been speculated that polymer properties like viscosity, chain orientation, interdiffusion rates, or mechanical properties and the glass transition temperature may change once the thickness of the film decreased below the diameter which Gaussian polymer coils have in bulk samples.

In Fig. 1.1 we show observations on changes in film thickness published already in 1993 [10]. There, annealing freshly spin-cast thin polymer films well below the glass transition temperature of the bulk system ($T_{g,bulk}$) for one hour under vacuum, followed by a quench to room temperature, showed significant increase in film thickness, i.e. a decrease in film density by X-ray reflectometry. It has to be emphasized that at these low temperatures well below $T_{g,bulk}$, no dewetting was observed. It also has to be noted that such films, when annealed (or aged) at temperatures well below $T_{g,bulk}$, showed a reversible behavior in the change of film

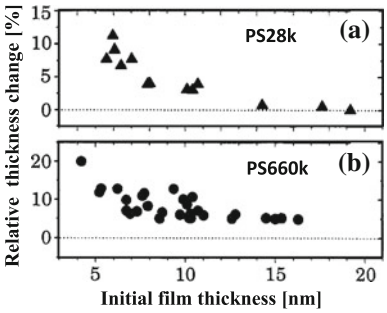

Fig. 1.1 Maximum relative change in thickness normalized by the initial thickness h_0 of the film as a function of h_0 for **a** polystyrene of M_w = 28 kg/mol (PS28 k) and **b** polystyrene of M_w = 660 kg/mol (PS660 k). The density of these films was lower than in the bulk and decreased with decreasing h_0. This change in density caused an increase of the mobility of the molecules with decreasing h_0. It was suggested that these effects resulted from an enlargement of the number of inaccessible sites caused by segregation of the molecules as h_0 decreased. The figure is adapted from Ref. [10]

thickness with temperature. The observed values of the relative change in film thickness decreased as h_0 increased. In addition, the observed thickness changes showed an influence of molecular weight.

From these observations, published in 1993 [10], it has been concluded that *"sufficiently thin films show, compared to the bulk, a lower density and an increased mobility. The latter corresponds to a reduction of the glass transition temperature which, in turn, can be related to the lower density."* As a tentative answer for the question "Why is the density of polymers confined in a thin film lower than that in the bulk?" it was speculated that *"chains do not significantly interpenetrate each other due to high entropy losses* [48], *the density of these swollen chains has to be lower than in the bulk. One might call the empty sites within the chains the <inaccessible volume>".*

Reflectometry studies of spin-cast thin polymer films [10–13, 20, 21, 23, 24] provided rather detailed information on changes in film thickness and interfacial roughness of the film/air interface. In particular, it was found that thin polymer films "shrink" by large amounts when annealed in the glassy state at temperatures even well below $T_{g,bulk}$. Changes in film thickness by more than 10 % have been observed at temperature well below $T_{g,bulk}$, even at room temperature when storing these films for days or months. This is not compatible with the assumption that polymer films are incompressible. Consequently, one has to anticipate that right after the film has been prepared by spin-casting, i.e. by rapid evaporation of the solvent, polymer films contained a large amount of unoccupied volume. Tentatively, one may assume that this then unoccupied volume was previously taken up by the solvent molecules which have evaporated from an already vitrified film. These observations of anomalously large thickness changes in ultra thin films of glassy polystyrene polymers have been summarized in [18] through a cascade of metastable states. There, also some (tentative) interpretations of these states, schematically shown in Fig. 1.2, have been suggested.

Unexpectedly, in several cases these films were not stable, i.e., dewetted and transformed into droplets, when annealed above $T_{g,bulk}$. Even more surprisingly, the thinnest films were unstable even below $T_{g,bulk}$ [10]. Stability, however, is a precondition for investigating specific properties as a function of film thickness.

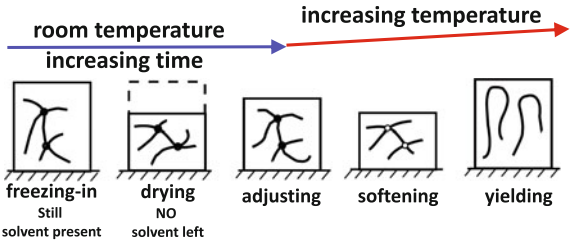

Fig. 1.2 Schematic presentation of some typical states of a spin-cast polymer film. While some initial processes may take place within seconds, subsequent relaxation and aging processes, in particular at temperatures below the glass transition temperature, may involve significantly longer times. The figure is adapted from Ref. [18]

For somewhat thicker films annealed at higher temperatures, but still well below $T_{g,bulk}$, simple inspection of these thin films by optical microscopy made it clear that the instability of the film was related to a retraction of the film from the substrate, i.e. the film dewetted the substrate [49]. The dewetting process provides profound insight into rheological properties of thin polymer films [32]. Polymers have negligible vapor pressure (polymers are non-volatile) which ensures mass conservation in the course of dewetting. Their typically rather high viscosity assures that dewetting is slow enough to allow for simple, time resolved measurements. Moreover, the possibility to tune the film thickness in the nanometer range allowes for testing the influence of short and long range intermolecular forces on film stability and dewetting dynamics [50–52]. Dewetting allows to investigate kinetic effects like friction (energy dissipation) at an interface. Dewetting experiments are attractive because of their simplicity, sensitivity and rapidity.

We conclude by stating that dewetting allows to link static and kinetic molecular and interfacial properties with macroscopically easily observable parameters like dewetting velocity and shape of the rim [47]. Despite its simplicity with respect to experimental observation, dewetting turned out to be extremely sensitive to even tiniest changes in the system under investigation. Thus, dewetting has proven to be a highly successful and time-efficient tool for obtaining time-resolved information on a molecular scale, allowing to determine interfacial properties and their changes in real time and in situ. Finally, dewetting experiments can provide information about relaxation and aging processes of polymers in the film.

1.3 Dewetting: Some Basic Features and Theoretical Considerations

In general, if a substrate has a lower surface tension than a fluid, this fluid will not form a stable film when deposited onto such a substrate. Consequently, such an unstable fluid film will retract from this substrate by a dewetting process [49, 53–57]. Capillary forces resulting from intermolecular interactions are responsible for this retraction of the fluid film [53]. The process can be described by the balance of driving forces, which try to remove the fluid, and dissipative processes, which reflect the resistance of the fluid to its removal. In particular, the temporal evolution of the dewetting process is controlled by this balance of forces.

In this context, it is an advantage that we are investigating thin films. Under such conditions, we can neglect gravity (because the mass of the film is extremely small) and inertia (because we investigate cases where the dewetting velocity is comparatively small). While many geometries and interfacial conditions can be considered, we concentrate on the simple case of a visco-elastic fluid on a smooth substrate. Accordingly, we assume that the fluid is completely characterized by its viscosity and elastic component. Moreover, we assume that the substrate is inert and does not generate hysteretic behavior, i.e., we exclude contact line pinning and chemical reactions at the substrate.

In Fig. 1.3, we define the central parameters, which have to be measured systematically in a dewetting experiment. The changes of the dewetted distance (this is either the radius $R(t)$ of a hole, when dewetting is initiated by a point, or the distance $L(t)$ to an initiating straight contact line) are controlled by the balance of acting forces, for example related to frictional properties at the film-substrate interface. The parameters $W(t)$ and $H(t)$, which characterize the rim, reflect information on the rheological properties of the fluid film.

As mentioned above, on non-wettable substrates, capillary forces are responsible for the retraction of a fluid film. These forces will also act if the film is vitrified or highly viscous, characterized by an elastic or visco-elastic behavior. Thus, one may expect that dewetting of visco-elastic films is following similar laws [58, 59]. Dewetting, however, may be slow or quasi-stopped on experimentally accessible time-scales if the acting forces are weak. In the following, we will discuss how visco-elastic properties of a film, and in particular stresses within the film, affect the dewetting process. For thin PS films the time-scale of such dewetting experiments is expected to be extremely long, especially at temperatures not too far above $T_{g,bulk}$ [19, 56, 57]. Furthermore, it may be questioned if capillary forces of the order of 10 mN/m are strong enough to provoke dewetting. In order to be able to observe dewetting within acceptable times, and to emphasize the consequences of driving forces, we have reduced interfacial friction by using low friction surfaces like silicon substrates coated with polydimethylsiloxane (PDMS). This allowed us to follow the process of hole growth in polystyrene (PS) films in detail across many length- and time-scales.

As one may have guessed, elasticity of the film is affecting characteristic features of the dewetting morphology. The dynamics of dewetting, i.e., the temporal

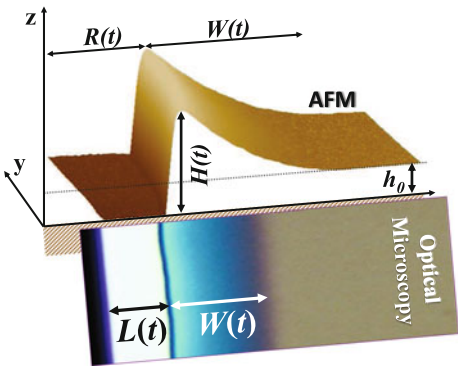

Fig. 1.3 Typical 3D view (measured by atomic force microscopy), compared with the observation by optical microscopy, of a section of a typical rim around a dewetting hole obtained in a PS film on a PDMS-coated substrate at temperatures close to the glass transition of PS. $H(t)$ is the maximum height of the rim which depends on dewetting time t. h_0 is the initial height of the film, $L(t)$ and $R(t)$ represent the dewetted distance for dewetting from a straight line or for the opening of a hole, respectively. $W(t)$ is the width of the rim. While h_0 and $H(t)$ are in the nanometer range, all other lengths are of the order of micrometers

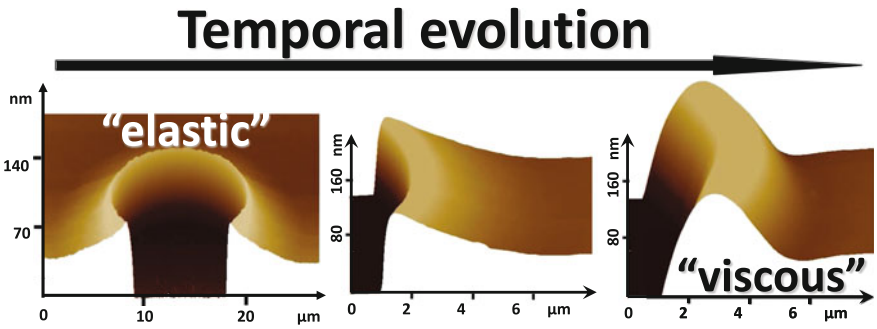

Fig. 1.4 3D-view (measured by atomic force microscopy) of a typical hole obtained by dewetting a polystyrene film on a PDMS-coated substrate at temperatures close to the glass transition of PS. The focus is on the evolution of the cross-section of the rim, which changes from an asymmetric shape at early stages to a more symmetric shape at late stages

evolution of the shape of the rim or the hole diameter is differing from purely Newtonian liquid films [58, 59]. For long dewetting times, however, even polystyrene films switch from an initially highly elastic behavior to a purely viscous fluid [60]. Visco-elastic fluids behave elastically at short time-scales and show viscous flow at long times. This change in rheological behavior becomes clearly evident in the dewetting features, e.g., represented by the shape of the rim, as can be seen in Fig. 1.4. Of course, the time of this transition depends on the characteristic relaxation time of the visco-elastic fluid, which typically decreases with increasing temperature.

1.4 Dewetting Experiments with Polystyrene Films at Temperatures Slightly Above the Glass Transition

A surprise and thus representing a significant result concerns dewetting of ca. 10–20 nm thin PS films of widely different molecular weight at temperatures around $T_{g,bulk}$ [19]. Like for dewetting at high temperatures, these films ruptured upon annealing. Here, we concentrate on the probability of hole formation and how these holes evolve with time at temperatures above ca. 103 °C. Complementary experiments indicated, however, that hole formation was possible at even lower temperatures [27].

In Fig. 1.5, we present typical atomic force microscopy (AFM) results for early stages of dewetting in very thin films. Many holes of similar size were formed within the small area detected by AFM [19]. Most holes were formed within a narrow time interval at the very beginning of annealing at 105 °C. At such early stages, the material displaced from the dewetted areas was not collected in visible rims around these areas but it was distributed evenly within the whole film in

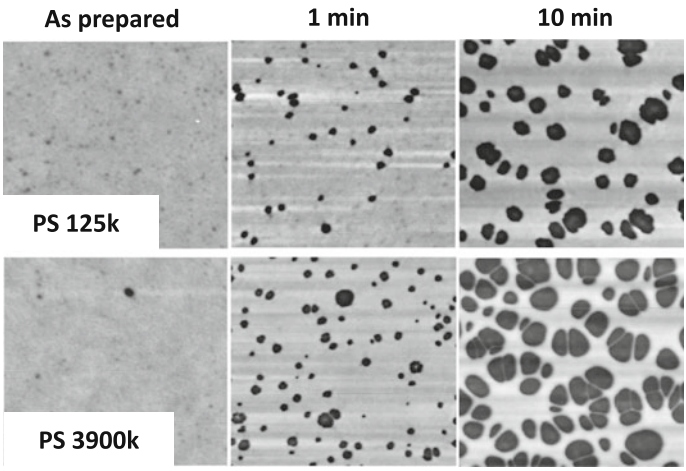

Fig. 1.5 Typical atomic force micrographs showing the consequences of annealing thin PS films on PDMS coated Si-wafers at a temperature close to the glass transition of PS. Rimless holes of some 100 nm in diameter were formed within minutes. Two different molecular weights are compared as indicated in the figure. First row: 16 nm polystyrene of M_w = 125 kg/mol (PS125 k); second row: 13 nm polystyrene of M_w = 3900 kg/mol (PS3900 k). First column: the as-prepared samples; second and third column: measured after annealing for 1 and 10 min at 105 °C, respectively. The size of the images is 3 × 3 μm^2. The figure is adapted from Ref. [19]

between the holes. Thus, imposing mass conservation, the film thickness between the holes had to increase, as was verified by AFM by measuring the depth of the holes.

The surprising aspects are twofold: First, independent of how long the polymers were, the rate of hole opening was almost identical. This implies that the viscosity of the polymer, which increases significantly with molecular weight and differed by many orders of magnitude for the two polymers investigated, was not the key rheological parameter characterizing the rate of hole opening. This result rather indicated that the plateau shear modulus of PS, which does not depend significantly on chain length, was the essential control parameter for the growth rate. Second, the initial opening velocity of the holes was of the order of 100 nm/min. For temperatures close to the glass transition with reptation times of the order of years, we cannot interpret the observed dewetting by viscous flow of the polymer. In addition, as could be deduced from the asymmetric shape of the rim observed for larger holes obtained in thicker PS films, the film behaved mainly like an elastic sheet. However, assuming a purely elastic material, the acting capillary forces, derived from known values of interfacial and surface tensions, would not be sufficient to lead to such an unexpectedly high dewetting velocity. Thus, it became obvious that an additional driving force was required.

Based on these experiments of 2001, it was concluded that a thin film does not need to be purely liquid in order to allow for dewetting. Also, thin solid films of low elastic modulus and large deformability can be dewetted, given that intermolecular

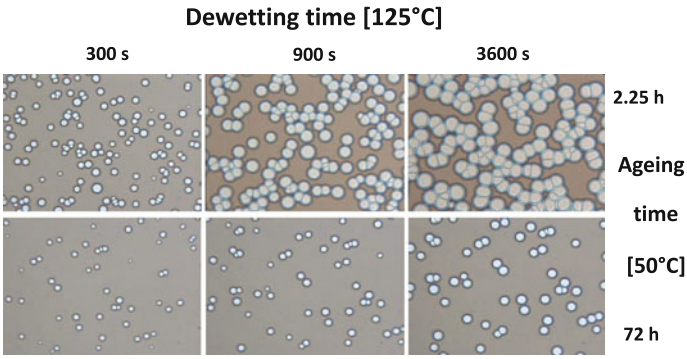

Fig. 1.6 A typical example showing the influence of aging at 50 °C on the probability of film rupture. The consequences of aging well below T_g were visualized by subsequent dewetting at 125 °C. Clearly, the number of holes and the diameter at a given time of dewetting decreased with aging time. The size of the images is 310 × 210 μm^2. The figure is adapted from Ref. [47]

forces are strong enough. Furthermore, it was stated in [19] that "phenomena like changes in film morphology or apparent thickening may also occur below the glass transition temperature (T_g) and can therefore not be taken as a criterion for determining T_g."

Some time later [28], the required additional driving force was identified through aging experiments (see Fig. 1.6): holes formed less rapidly and less frequently in films which were stored for some time (days up to years) at room temperature. Thus, it was speculated that polymers within a thin spin-cast film experience internal tensions (residual stresses) which relaxed during aging. It was assumed that these residual stresses were induced during sample preparation and attributed to the fact that the polymers were confined to thin films, which sometimes were even thinner than the size of the unperturbed coil.

Intriguingly, as e.g. clearly shown by the diameter of the holes after one hour of dewetting, aging for only a few hours at temperatures well below T_g caused dramatic changes in the dewetting behavior. Thus, even in the glassy state the induced stresses were able to relax, at least partially. This reduction of stresses occurred at an unexpectedly fast rate, given that no long range movements of the polymers are possible in the glassy state.

1.5 Consequences of Transient Residual Stresses in Thin Polymer Films

The relaxation process of residual stresses can also be followed indirectly by studying dewetting of spin-cast thin viscoelastic polymer films on soft elastic substrates [33]. There, the transient contribution of residual stresses leads to a nonmonotonic, two-stage dewetting behavior (see Fig. 1.7). The magnitude of the

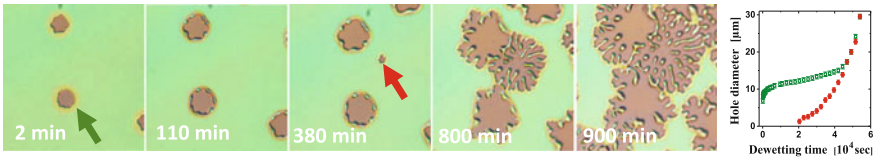

Fig. 1.7 Optical micrographs showing dewetting of a 40 nm PS film (M_w = 1.0 Mg/mol) on a 200 nm PDMS layer at 180 °C for increasing time. The size of the images is 58 × 58 μm^2. The graph at the end represents the hole diameter (for uneven holes, a mean diameter of the enveloping perimeter of the hole was taken for a hole starting to grow immediately (labeled by a *gray arrow*) and a hole (labeled by a *dark arrow*) starting to grow with a delay of several times the reptation time. The figure is adapted from Ref. [33]

residual stresses, introduced by out-of-equilibrium molecular conformations, can amount up to several times the capillary force [31, 61, 62]. In these dewetting experiments, part of the corresponding energy of the residual stresses is temporarily stored in the form of deformation energy of an elastic substrate. The size of this deformation is thus making the magnitude of these stresses visible.

Due to the formation of an elastic deformation of the substrate (the trench), achieved after only few minutes of annealing at 140 °C (see Fig. 1.8), hole opening came to an apparent standstill. The forces resisting dewetting due to the elastic trench remained until polymer diffusion and viscous flow were able to equilibrate the trench. This equilibration needed times of the order of the reptation time and led to the formation of a much shallower "viscous trench" caused by the normal component of the capillary force. At that point, most resistance due to deformation of the rubbery PDMS film was removed and the PS film slipped on the PDMS substrate.

The substrate depression (D), measured inside the hole (see Fig. 1.8f), was considered as a direct indicator of the local strain in the PDMS layer, from which the total dewetting force exerted on the film was estimated [28, 32, 58, 59]. D reached a maximum value within relatively short time and slowly started to decrease afterward (see Fig. 1.8g). The maximum value of D, but also the size of the maximum (quasistatic) hole diameter, which also was reached rapidly in times much shorter than the reptation time (τ_{rep}), were found to be largely independent of molecular weight for the high molecular weight samples studied.

In conclusion, at times shorter than the relaxation time of the polymer (i.e., $t < \tau_{rep}$), dewetting generated deep trenches in the soft rubbery substrate which, in turn, almost stopped dewetting. At later stages ($t > \tau_{rep}$), dewetting accelerated, accompanied by an unstable rim. However, when holes were nucleated only after the relaxation of residual stresses, they never caused large deformations of the soft substrate. There, no significant elastic trench was formed and equilibration of the trench was fast. The transition to a viscous dewetting behavior occurred soon after hole nucleation. Thus, the observation of two stages in the dewetting process is

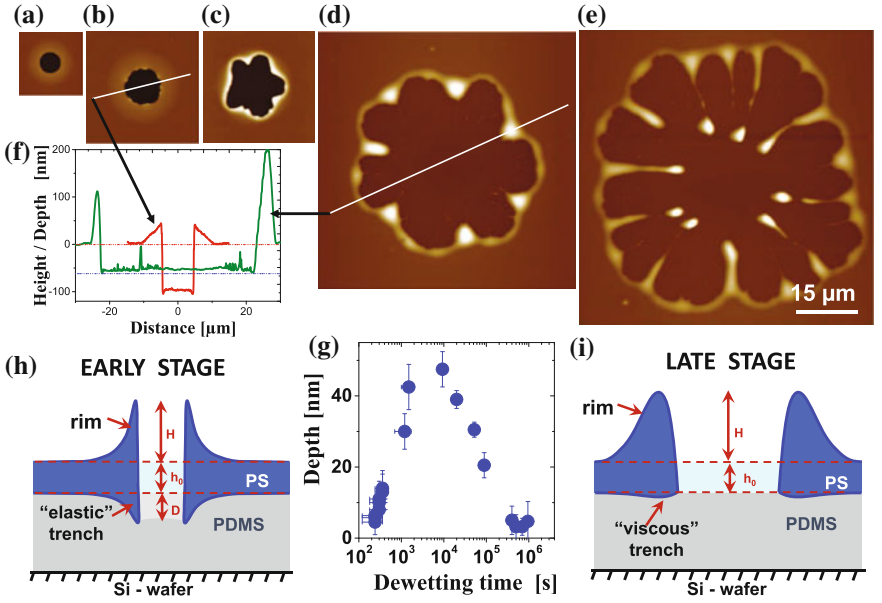

Fig. 1.8 Atomic force microscopy dewetted holes in a 55 nm PS film (M_w = 1.0 Mg/mol) on a 360 nm PDMS layer, dewetting at 140 °C (τ_{rep} = 160000 s) for **a** 300, **b** 1500, **c** 20 000, **d** 800 000, and **e** 950 000 s, respectively. **f** Cross sections indicated by white lines through holes (**b**) and (**d**). The surface of the unperturbed PS film has been set to zero depth level. Accordingly, the level of the unperturbed PDMS surfaces is at 55 nm below the unperturbed PS surface. The trace through the hole (**b**) represents the transient depression of depth D in the soft substrate. **g** Depth of the depression within the hole versus dewetting time for the sample shown in **a**–**e**. **h** and **i**: Schematic representation of the shape of the rim and the trench of a dewetting hole in a PS film deforming the soft rubbery PDMS layer underneath. Because of elastic deformation of the PS film at early stages the corresponding elastic trench is digging into the soft PDMS under-layer quite deeply. At late stages, after the relaxation time τ_{rep}, only a small deformation (viscous trench) due to the normal component of the capillary force at the three phase contact line is left in the PDMS layer. The figure is adapted from Ref. [33]

attributed to large elastic deformations in the substrate which are caused by transient residual stresses within the film.

If stresses would not relax and the elastic deformation of the substrate could be maintained indefinitely, holes would never grow beyond a maximum diameter determined by the balance of forces driving dewetting and the counteracting elastic force resulting from the induced elastic deformation of the rubbery substrate. Thus, the slow disappearance of such elastic behavior in the course of time demonstrates the existence of long-lasting, but nonetheless transient metastable states within spin-cast thin polymer films.

1.6 Aging and Relaxation Processes of Residual Stresses in Thin Polymer Films

The non-equilibrium properties of spin-cast polymer films manifest themselves also in the hole-opening kinetics [38, 45]. Because the effects introduced by film preparation may change with time, special care must be taken when conducting hole-opening experiments: Since PS films are known to change their properties when stored at room temperature (aging), the time elapsed between film preparation and the beginning of the dewetting experiment must be taken into account. When brought to the dewetting temperature (above T_g), holes nucleate at various times during annealing. Dewetting of holes nucleated after some incubation time are thus reflecting the behavior of an already (partially) annealed film with no or with reduced residual stresses. As can be seen in Fig. 1.9a, we can follow simultaneously the temporal evolution of several holes, nucleated after different incubation times. While all holes show qualitatively a similar behavior (see Fig. 1.9b), the superposition of these curves as a function of the time for which they actually grew (see Fig. 1.9c) shows significant slowing down of growth with incubation time,

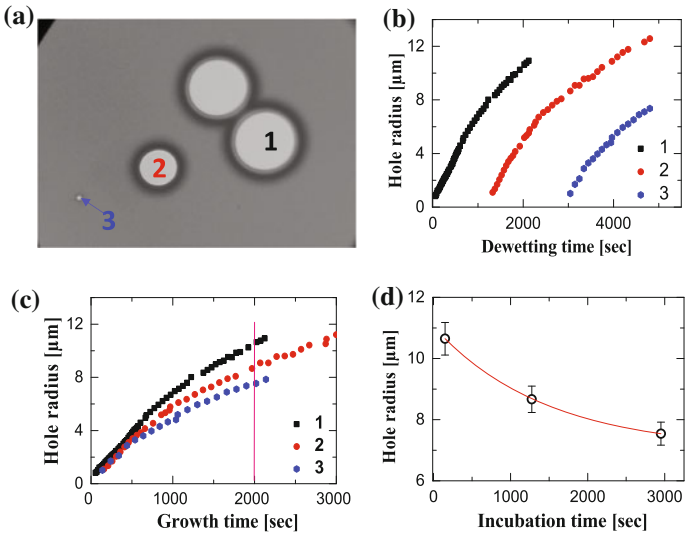

Fig. 1.9 **a** Optical micrograph (size: 143 × 106 µm^2) of a PS film (M_w = 16800 kg/mol, thickness is ca. 40 nm) cast from toluene at 23 °C, after heating for 53 min at 125 °C. Smaller holes were nucleated after longer incubation times compared to the bigger holes nucleated at earlier times. **b** Growth of the three holes marked 1, 2, and 3 in **a**, which were nucleated 90, 1275, and 2950 s after the film was brought to 125 °C. **c** Growth of the same holes where the ordinate is the time that each hole has grown since it was nucleated, rather than the time elapsed since the film reached T = 125 °C. **d** Plot of the hole radii of the three holes after a growth time of 2000 s (*vertical line* in (**c**)), showing an exponential decay with a time constant of 1000 ± 500 s. The figure is adapted from the doctoral thesis of Mithun Chowdhury (2012)

following approximately an exponential decay (see Fig. 1.9d, yielding a characteristic decay time of 1000 ± 500 s). This clearly demonstrates that in the course of annealing the contribution of residual stresses to the driving force has decayed, indicating that the out-of-equilibrium chains in the films (partially) relaxed during annealing in the course of the dewetting process. Note that the decay time deduced in Fig. 1.9d is much smaller than the bulk reptation time at the dewetting temperature ($\tau_{rep} \approx 2 \cdot 10^8$ s [32] for the high molecular weight PS used here).

Obviously, non-equilibrated films will evolve towards equilibrium causing a change in film properties with time. However, when films are kept at temperatures below the glass transition, it is not clear whether significant and detectable changes can occur on experimentally accessible time scales. Under such conditions of aging, relaxations on the level of entire chains are not expected. Rather, local motion at the level of chain segments are possible, characterized, e.g., by the β-relaxation [63, 64]. This raises the question, whether such segmental relaxations have an impact on static and dynamic properties of polymers observed at a macroscopic level, for example, through changes in film thickness or the dynamics of dewetting.

Furthermore, it is not clear whether the presence of residual stresses, caused by strong deviations of chain conformations from equilibrium, accelerate or slow down relaxations at the segmental level. Thus, we have investigated the consequences of physical aging in thin spin-cast polystyrene films through detailed dewetting studies [38, 45], focusing on the relaxation dynamics during aging of the glassy film. We detected changes induced by aging below $T_{g,bulk}$ through systematic variations of the duration and the temperature of aging. A simultaneous study of different observables (diameter of the dewetting hole, and shape and size of the rim formed during dewetting) enabled us to exclude purely interfacial phenomena and to relate the relaxations to changes occurring within the entire film. From these observations, we were able to deduce the relaxation dynamics, i.e., the decay time of residual stresses inside the film as a function of aging temperature.

The temporal evolution at the early stages of hole formation was followed in real time by optical microscopy and, after quenching the dewetted films to room temperature, height profiles of the rim were measured by atomic force microscopy (AFM). We note that only holes detectable immediately after initiating dewetting were investigated. Thus, the opening of all holes was subject to the same residual stress. Figure 1.10a displays typical images characteristic for the influence of aging on the dewetting dynamics. For a fixed dewetting time for each sample, the hole radius R, the width W, and the height H of the rim decreased upon physical aging at 80 °C with increasing aging times. As shown for aging at 25 °C in more detail in Fig. 1.10b, R increased more slowly the longer the film was aged. This effect was more pronounced, i.e., less time was needed to achieve the same amount of changes, at high aging temperatures. From such aging experiments we thus can deduce a temperature dependent decay time τ_A, simultaneously for the evolution of R, W, and H. The values of τ_A, deduced from the exponential decay of the dewetting velocity, the width, and the height of the rim with aging time were found to be rather equal. Independent of aging-temperature, the determined values of τ_A,

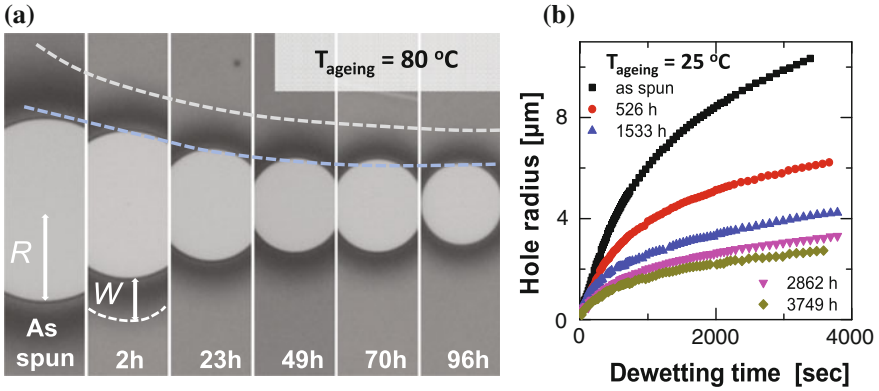

Fig. 1.10 **a** Section of dewetting holes in nominally identical PS films (thickness 40 ± 2 nm, M_w = 4060 kg/mol) that have been aged at 80 °C for varying periods ranging from 2 to 96 h, taken after dewetting at 125 °C for ca. 1 h. The size of the optical micrographs is ca. 14 × 60 μm^2 each. **b** Temporal evolution of the radius of dewetting holes, nucleated immediately upon heating to 125 °C in PS films (40 ± 2 nm, 4060 kg/mol) that have been aged at 25 °C. At any fixed dewetting time (for example at 1000 s), both the hole radius and its growth velocity (derivative of the radius with respect to dewetting time) exhibited a decrease with aging time. The figure is adapted from Ref. [45]

characterizing the relaxation of residual stresses inside the film caused by out-of-equilibrium chain conformations induced by the spin-casting process [28, 32], were smaller than τ_{rep}.

In an analogous series of experiments, we measured the characteristic decay time with aging time at room temperature for thin films cast from solutions of strongly differing quality of the solvent. We used trans-decalin as solvent which has a Θ-temperature of ≈21°C. In Fig. 1.11a, we schematically indicate how the coil diameter in solution varied with the temperature of the solution from which the films were cast. As can be seen from Fig. 1.11b, varying the temperature of the spin-casting solution has a substantial effect on the room temperature relaxation times of these films. Comparing both, the variation of the relaxation time and the coil diameter as a function of spin-casting temperature, clearly shows that both follow the same trend.

While the coil diameter changes only little as the solution is becoming more concentrated in the course of solvent evaporation, the coil volume is increasingly interpenetrated by other chains. The segmental mobility is, however, simultaneously reduced and is arrested when the solution reaches the glass transition temperature. With a lack of segmental mobility, further solvent evaporation leads to a collapse of the chains onto themselves. In a thin film, this collapse is restricted to one dimension, resulting in oblate coil structures. The deformation of the coil structure gives rise to an in-plane stress, while the reduction in entanglements lower the elastic modulus and the melt viscosity [37].

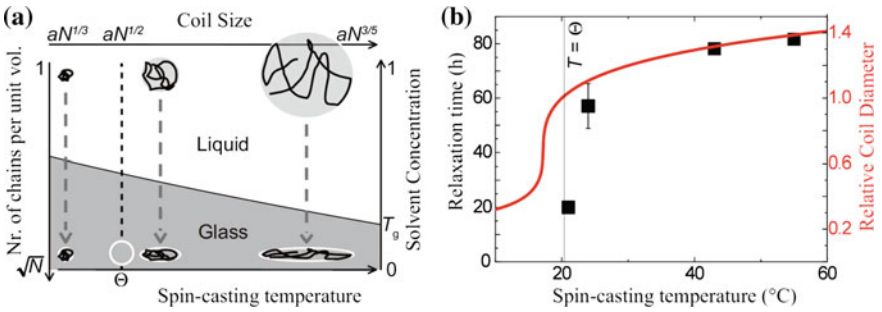

Fig. 1.11 **a** Schematic of polymer coil conformations upon spin-coating for temperatures above and below Θ-temperature. The *open circle* indicates a fully entangled chain in equilibrium. **b** Relaxation times τ_A as a function of the temperature of the solution from which the films were spun. The curve represents the result of the calculation of the coil diameter (end-to-end distance of the polymer coil) as a function of temperature with respect to Θ of PS in trans-decalin (indicated by the *vertical dotted line*), with the concentration as a fitting parameter. The variation of the solution temperature thereby provides control over the swelling of PS chains in the solution over a considerable range, given by [65]. The figure is adapted from Ref. [38]

Figure 1.11b shows that the quality of the solvent from which polymer films are cast plays a significant role in determining the aging behavior of the non-equilibrium conformations of the chains in the film. Interestingly, the aging time increases with improving solvent quality, with the strongest effect observed for the athermal solvent. Faster stress relaxation does, however, not necessarily imply a faster overall equilibration of the chains. Full equilibration is likely to be of the same order of magnitude as the bulk (equilibrium) reptation time.

In Fig. 1.12a we show the temperature dependence of the characteristic relaxation times (τ_A) upon aging as extracted from the dynamics of R, W, and H, demonstrating that all three observables yielded quantitatively similar behavior. These results clearly indicate that the dynamics of all dewetting observables is governed by the same physical parameters. As changes in interfacial properties (friction with the substrate) are not expected to cause a change in H, the similar decay of all three quantities strongly points to a relaxation process occurring within the entire film.

The only dewetting parameter which affects all three quantities in a similar way is the ratio of the total stress acting at the contact line over the elastic modulus of the film. Thus, the relative decay of H during aging can either be due to a decay of residual stress (assuming that the capillary stress is constant and interfacial tensions do not significantly change with aging), or be caused by an increase in the elastic modulus [32, 58, 59]. The latter requires, however, the formation of a significant number of new entanglements during the course of aging. Below the glass transition temperature, chain reptation is suppressed and entanglement formation is extremely unlikely. Intrachain segmental motions are however still possible. Thus, the simultaneous and equally fast decay of all three observables can only be attributed to a decay of residual stress, and consequently, to relaxations at a segmental level.

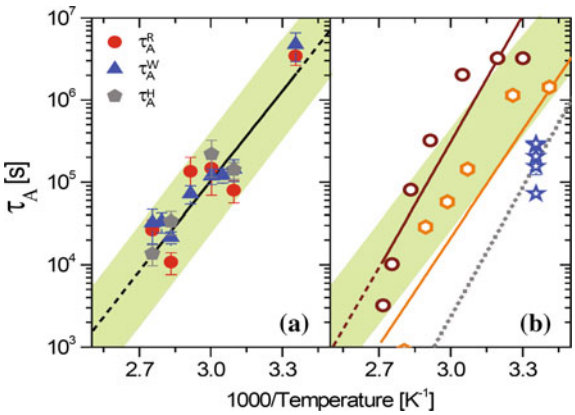

Fig. 1.12 **a** Relaxation times (τ_A) deduced from the evolution of the hole radius, the maximal rim width, and the rim height, respectively, vs. inverse aging temperature, of nominally identical PS films (M_w = 4060 and 4840 kg/mol) prepared by spin-casting from toluene. The *solid line* is an Arrhenius fit of all relaxation times, yielding an activation energy E_a = 70 ± 6 kJ/mol. The highlighted area encompassing all data points and their *error bars* gives rise to a range in E_a values between 50 and 107 kJ/mol. **b** Comparison of the results of **a** (*shaded area*) with reported relaxation times derived from the surface relaxations of (i) nano deformations (*open hexagons*) [34] and (ii) nano bumps (*open circles*) [46], including Arrhenius fits to these data (*solid lines*). The *dotted line* represents results from dye probe reorientation measurements [44] and *the stars* show relaxation times for PS films spun from trans-decalin [38]. The figure is adapted from Ref. [45]

The results of Fig. 1.12a suggest an Arrhenius behavior for the relaxation time

$$\tau_A = A_0 \exp\left(\frac{E_a}{k_B T}\right), \tag{1.1}$$

where A_0 is a constant, k_B is the Boltzmann constant and E_a is the activation energy of the underlying relaxation process. From a fitting to our results we obtain E_a = 70 ± 6 kJ/mol.

It is instructive to compare this value derived from a macroscopic dewetting study to the β-relaxation process, which is believed to involve non-cooperative motions at the segmental level of the polymer chain [63, 64]. In the literature, values of 150 ± 80 kJ/mol for the β-relaxation in thin film and bulk PS can be found [14, 63, 64, 66]. Similar values were also found when measuring the kinetics of irreversible chain adsorption [67].

Several studies on thin polymer films also indicated a sub-T_g Arrhenius-type relaxation process, which was related to the motion within a distinct surface layer of higher mobility or to increased heterogeneity [35, 44, 63, 64], yielding $E_a \approx$ 100 kJ/mol [44] and E_a = 185 ± 3 kJ/mol [14]. Lateral force microscopy measurements on thin PS films [63] found a thickness dependent surface β-relaxation process, with E_a = 55 kJ/mol for a 65 nm thick film. Fast sub-T_g-relaxations at surfaces of thin polymer films were measured by AFM, including the relaxation of

surface dimples (E_a = 83 ± 16 kJ/mol) [34] and the reduction in the height of surface bumps in water (E_a = 98 ± 17 kJ/mol) [46]. Interestingly, within the scatter of the data, our results exhibit the same order of magnitude in relaxation time as these surface relaxation processes, cf., Fig. 1.12b.

Dewetting is not a surface sensitive technique. In particular, the height of the rim is not controlled by a possible high mobility surface layer. Dewetting involves the displacement of whole polymer chains and takes place across the entire film thickness. Moreover, at the used dewetting temperature, the film behaved like an elastic body, as demonstrated by the asymmetric shape of the rim. Stress relaxation could therefore, only occur by motion on the level of chain segments.

Furthermore, it is illuminating to compare room temperature relaxation times shown in Fig. 1.11b for aging films spun from different solvents (see stars in Fig. 1.12b. A reduction in solvent quality gave rise to a decrease in relaxation times, indicating that the state of polymer chain entanglement in solution was transferred to the dried film [38]. The change from a good solvent (toluene) to a near-θ solvent (transdecalin) corresponds to a decrease in chain swelling (radius of gyration) in solution, leading to reduced chain overlap and thus to a decrease in observed relaxation times. These results indicate that segmental relaxation depends on the local chain environment, which is strongly affected by preparation conditions such as solvent quality and film deposition technique.

In conclusion, the experiments presented here suggest that motion on the level of chain segments is sufficient to partially relax frozen-in out-of-equilibrium local chain conformations, which are the cause of residual stresses in thin polymer films. These relaxations are not expected to fully equilibrate the polymer film, which would require reptation of entire chains. It is also unlikely that segmental rearrangements lead to a homogeneous system on a nanometer length-scale. It is interesting and surprising to discover that changes in PS surface topography and the here studied influence of aging on dewetting exhibit similar relaxation times and rather similar activation energies. This might indicate that segmental relaxations are responsible for both observations. However, further studies are needed to answer the question whether local changes at the level of chain segments are responsible for changes in the surface topography on length-scales which are several orders of magnitude larger than the size of the relaxing segments. In film dewetting, however, such local rearrangements have a dramatic influence, revealing the effect of submolecular (segmental) processes on macroscopic length-scales. Our results further suggest that rearrangements at the level of chain segments are sufficient to partially relax frozen-in out-of-equilibrium local chain conformations, i.e., the cause of residual stresses, and they might also be responsible for macroscopic relaxations at polymer surfaces.

Finally, the strong dependence of the aging behavior of thin films far below T_g on film preparation conditions sheds a new light on the low temperature softening of thin polymer films (that is their lowered glass transition temperature). While the deformation of polymer coils as a whole should not modify the solidification temperature of the film, which is dominated by the segmental dynamics, our aging experiments indicate that spin-coating perturbs the polymer coils down to the

segmental length scale. While this needs further experimental verification, our experiments point towards an explanation for the "abnormal" glass transition temperature in thin films in terms of non-equilibrium chain conformations caused by film preparation.

1.7 Concluding Remarks

For achieving functional macromolecular systems with adaptable properties engineered via processing, we need to establish fundamental understanding of generic processes of polymer (re-)organization and rearrangements during the various processing steps, all causing potentially chain conformations (far) **beyond** thermodynamic equilibrium, characterized e.g. by a Gaussian chain statistics representing the minimum of free energy. Based on such insight, a rational design of the processing steps will be possible and so macromolecular systems can be achieved which have unprecedented and adaptable (improved) mechanical, optical, surface, … properties.

Non-equilibrium states are often anisotropic and consist of preferentially oriented/aligned polymer chains. Thus, under appropriate processing conditions, these non-equilibrium states represent, or evolve into, ordered structures and metastable states, which exhibit properties not achievable under equilibrium condition. For example, changes at the conformational level of polymers may lead to macroscopic changes in behaviour, e.g. represented by changes in the glass transition temperature.

The difference in energy of various non-equilibrium states is often extremely small which enables large deformability of polymers at rather low energetic costs. For example, by changing their conformation from a coiled state to a largely extended state, macromolecules are highly suitable to flow under extreme conditions (high shear rates, large deformations) without leading to macroscopic disintegration. Corresponding low molecular weight systems would often not be homogeneously processable under such extreme conditions. The dynamics of the resulting non-equilibrium states can deviate strongly (by many orders of magnitude!) from the behavior of the same polymers in the equilibrium state.

An equilibrated system, which is "dead" in the sense that, after a small perturbation, it will always try to return to a stable and well defined equilibrium state of lowest free energy. By contrast, non-equilibrated systems can explore a large variety of energetically similar non-equilibrated states: Switching between such states provides a possibility for adaption. For example, a semi-crystalline polymer material may respond to a mechanical deformation not only be relaxing back to the initial state but may alternatively form crystalline nuclei facilitated by a shear-induced reduction of the nucleation barrier. In such a case, the growth of crystalline domains (lamellae) will be in the direction orthogonal to the direction of the applied force. Thus, as an attempt to avoid e.g. damage through the applied force, such materials may potentially exhibit a self-enforcing capability of their

mechanical properties, in some sense similar to biological (plant) systems. Crystallization is also a well suited example for how changes at the level of the monomer (e.g. through variations in side-groups) can affect order and the thereof derived properties. Taking advantage of the high degree of polymerization, changes at the level of a monomer are "multiplied" by the number of monomers connected in the polymer chain. Thus, by synthesizing/designing appropriate monomers one may achieve a massive amplification and control of the above-mentioned structure formation processes during processing.

Acknowledgments I am highly indebted to Françoise Brochard and the late Pierre-Gilles de Gennes for many invaluable discussions. I wish to thank Rajesh Khanna, Samer Al Akhrass, Pascal Damman, Mithun Chowdhury, Ulli Steiner, Thomas Vilmin, Falko Ziebert, and Elie Raphaël for the fruitful collaborations which are at the base of the here presented results. I am grateful to the Deutsche Forschungsgemeinschaft (RE2273/3-1) for funding of the most recent part of this work and partial financial support from the European Community's Marie-Curie Actions" under contract MRTN-CT-2004-504052 [POLYFILM] for the earlier stage of the work.

References

1. Keller, A., Odell, J.A.: Colloid Polym. Sci. **263**, 181 (1985)
2. Bernardin III, F.E., Rutledge, G.C.: Polymer **48**, 7211–7220 (2007)
3. Müller, de Pablo, J.J.: Annu. Rev. Mater. Res. **43**, 134 (2013)
4. Sprakel, J., Padding, J.T., Briels, W.J.: EPL **93**, 58003 (2011)
5. Huang, C.C., Winkler, R.G., Sutmann, G., Gompper, G.: Macromolecules **43**, 10107 (2010)
6. Mizunoa, H., Yamamoto, R.: Eur. Phys. J. E **35**, 29 (2012)
7. Croll, S.G.: J. Appl. Polym. Sci. **23**, 847858 (1979)
8. Bornside, D., Macosko, C., Scriven, L.J.: Imag. Technol. **13**, 122128 (1987)
9. Karpitschka, S., Weber, C.M., Riegler, H.: http://arxiv.org/abs/1205.3295
10. Reiter, G.: Europhys. Lett. **23**, 579–584 (1993) (Macromolecules **27**, 3046–3052 (1994))
11. Orts, W.J., van Zanten, J.H., Wu, W.L., Satija, S.K.: Phys. Rev. Lett. **71**, 867–870 (1993)
12. Sanyal, M.K., Basu, J.K., Datta, A., Banerjee, S.: Europhys. Lett. **36**, 265–270 (1996)
13. Bollinne, C., Cuenot, S., Nysten, B., Jonas, A.M.: Eur. Phys. J. E **12**, 389–395 (2003)
14. Yang, Z., Fujii, Y., Lee, F.K., Lam, C.H., Tsui, O.K.C.: Science **328**, 1676 (2010)
15. Keddie, J., Jones, R.A.L., Cory, R.: Europhys. Lett. **27**, 59 (1994)
16. Dalnoki-Veress, K., Nickel, B., Roth, C., Dutcher, J.: Phys. Rev. E **59**, 21532156 (1999)
17. Brulet, A., Boue, F., Menelle, A., Cotton, J.P.: Macromolecules **33**, 9971001 (2000)
18. Reiter, G., de Gennes, P.G.: Eur. Phys. J. E **6**, 2528 (2001)
19. Reiter, G.: Phys. Rev. Lett. **87**, 186101 (2001)
20. Mukherjee, M., Bhattacharya, M., Sanyal, M.K., Geue, T., Grenzer, J., Pietsch, U.: Phys. Rev. E **66**, 061801 (2002)
21. Kanaya, T., Miyazaki, T., Watanabe, H., Nishida, K., Yamana, H., Tasaki, S., Bucknall, D.B.: Polymer **44**, 3769–3773 (2003)
22. Efremov, M., et al.: Phys. Rev. Lett. **91**, 085703 (2003)
23. Miyazaki, T., Nishida, K., Kanaya, T.: Phys. Rev. E **69**, 022801 (2004)
24. Bhattacharya, M., Sanyal, M.K., Geue, T., Pietsch, U.: Phys. Rev. E **71**, 041801 (2005)
25. Si, L., Massa, M.V., Dalnoki-Veress, K., Brown, H.R., Jones, R.A.L.: Phys. Rev. Lett. **94**, 127801 (2005)
26. O'Connell, P.A., McKenna, G.B.: Science **307**, 1760 (2005)
27. Roth, C.B., Deh, B., Nickel, B.G., Dutcher, J.R.: Phys. Rev. E **72**, 021802 (2005)

28. Reiter, G., Hamieh, M., Damman, P., Sclavons, S., Gabriele, S., Vilmin, T., Raphaël, E.: Nat. Mater. **4**, 754 (2005)
29. Bodiguel, H., Fretigny, C.: Eur. Phys. J. E **19**, 185 (2006)
30. Peter, S., Meyer, H., Baschnagel, J.: J. Polym. Sci. B Polym. Phys. **44**, 2951–2967 (2006)
31. Yang, M.H., Hou, S.Y., Chang, Y.L., Yang, A.C.M.: Phys. Rev. Lett. **96**, 066105 (2006)
32. Damman, P., Gabriele, S., Sclavons, S., Desprez, S., Villers, D., Vilmin, T., Raphaël, E., Hamieh, M., Al Akhrass, S., Reiter, G.: Phys. Rev. Lett. **99**, 036101 (2007)
33. Al Akhrass, S., Reiter, G., Hou, S.Y., Yang, M.H., Chang, Y.L., Chang, F.C., Wang C.F., Yang, A.C.M.: PRL **100**, 178301 (2008)
34. Fakhraai, Z., Forrest, J.: Science **319**, 600 (2008)
35. Fukao, K., Koizumi, H.: Phys. Rev. E **77**, 021503 (2008)
36. Serghei, A., Kremer, F.: Macrom. Chem. Phys. **209**, 810–817 (2008)
37. Barbero, D.R., Steiner, U.: Phys. Rev. Lett. **102**, 248303 (2009)
38. Raegen, A., Chowdhury, M., Calers, C., Schmatulla, A., Steiner, U., Reiter, G.: Phys. Rev. Lett. **105**, 227801 (2010)
39. Roth, C.B.: J. Polym. Sci. B: Polym. Phys. **48**, 25582560 (2010)
40. Tress, M., Erber, M., Mapesa, E.U., Huth, H., Müller, J., Serghei, A., Schick, C., Eichhorn, K.-J., Voit, B., Kremer, F.: Macromolecules **43**, 99379944 (2010)
41. Napolitano, S., Pilleri, A., Rolla, P., Wübbenhorst, M.: ACS Nano **4**, 841–848 (2010)
42. Reiter, G., Napolitano, S.: J. Polym. Sci. B: Polym. Phys. **48**, 2544 (2010)
43. Napolitano, S., Wübbenhorst, M.: Nat. Commun. **2**, 260 (2011)
44. Paeng, K., Swallen, S.F., Ediger, M.D.: J Am Chem Soc **133**, 84448447 (2011) (Paeng K, Richert R, Ediger MD: Soft Matter **8**, 819 (2012))
45. Chowdhury, M., Freyberg, P., Ziebert, F., Yang, A.C.M., Steiner, U., Reiter, G.: PRL **109**, 136102 (2012)
46. Siretanu, I., Chapel, J.P., Drummond, C.: Macromolecules **45**, 10011005 (2012)
47. Reiter, G.: Glass transition, dynamics and heterogeneity of polymer thin films. In: Kanaya T (ed) Adv. Polym. Sci. **252**, 29 (2013)
48. Carmesin, I., Kremer, K.: J Phys (Paris) **51**, 915 (1990)
49. Reiter, G.: Phys. Rev. Lett. **68**, 75 (1992) (Langmuir **9**, 1344 (1993))
50. Brochard-Wyart, F., Daillant, J.: Can. J. Phys. **68**, 1084 (1990)
51. Herminghaus, S.: Phys. Rev. Lett. **83**, 2359 (1999)
52. Reiter, G., Khanna, R., Sharma, A.: Phys. Rev. Lett. **85**, 1432 (2000)
53. de Gennes, P.G., Brochard-Wyart, F., Quéré, D.: Gouttes bulles perles et ondes, Belin, Paris OR: Capillarity and Wetting Phenomena: Drops Bubbles Pearls Waves, Springer, Heidelberg (2002)
54. Redon, C., Brochard-Wyart, F., Rondelez, F.: Phys. Rev. Lett. **66**, 715 (1991)
55. Brochard-Wyart, F., Martin, P., Redon, C.: Langmuir **9**, 3682 (1993)
56. Krausch, G.: J. Phys.: Condens. Matter **9**, 7741 (1997)
57. Seemann, R., Herminghaus, S., Jacobs, K.: Phys. Rev. Lett. **87**, 196101 (2001)
58. Vilmin, T., Raphaël, E.: Eur. Phys. J. E. **21**, 161 (2006)
59. Ziebert, F., Raphaël, E.: Phys. Rev. E **79**, 031605 (2009)
60. Gabriele, S., Sclavons, S., Reiter, G., Damman, P.: Phys. Rev. Lett. **96**, 156105 (2006)
61. Thomas, K.R., Steiner, U.: Soft Matter **7**, 7839 (2011)
62. McGraw, J.D., Fowler, P.D., Ferrari, M.L., Dalnoki-Veress, K.: Eur. Phys. J. E **36**, 7 (2013)
63. Akabori, K.I., Tanaka, K., Kajiyama, T., Takahara, A.: Macromolecules **36**, 4937 (2003)
64. Lupasçu, V., Picken, S.J., Wübbenhorst, M.: J. Non-Cryst. Solids **352**, 5594 (2006)
65. Sun, S., et al.: J. Chem. Phys. **73**, 5971 (1980)
66. Dhinojwala, A., Wong, G., Torkelson, J.: J. Chem. Phys. **100**, 6046 (1994)
67. Housmans, C., Sferrazza, M., Napolitano, S.: Macromolecules **47**, 3390 (2014)